A Theoretical Study of the Structure and Spectra of Nitric Acid Hydrates Crystals

Delia Fernández, Vicente Botella,† Víctor J. Herrero, and Rafael Escribano*

Instituto de Estructura de la Materia, Consejo Superior de Investigaciones Científicas (CSIC), Serrano 123, 28006 Madrid, Spain

Received: January 29, 2003; In Final Form: July 1, 2003

Crystals of nitric acid hydrates have been studied theoretically by means of a recently developed ab initio method (SIESTA). Using as input data the X-ray structures of crystals of nitric acid monohydrate (NAM), dihydrate (NAD), and trihydrate (NAT), the atomic geometry within each unit cell has been refined. The calculated geometrical structure of these atmospherically relevant systems allows the study of further physicochemical properties. In this article, their vibrational normal modes have also been evaluated. These have been used to propose the assignment of the observed spectra of the hydrate crystals, with good overall agreement between experiment and calculation. This is the first time that this type of calculation has been carried out for NAD, whose recently observed two phases (I and II) have been studied here.

Introduction

The relevance of polar stratospheric clouds (PSC) in atmospheric chemistry has been established for some time (see for example, refs 1−3). This has prompted a large number of studies on their physical and chemical structure (refs 4−8 and references therein). Type I PSCs consist of mixtures of water and nitric acid, eventually with sulfuric acid as well, at different concentrations, in solid or liquid state, depending on pressure, temperature, and humidity.[9,10] Although nitric acid trihydrate (NAT) is the main component, the presence of the dihydrate (NAD) in the clouds is still under discussion. Both these species plus the monohydrate (NAM) are the subject of study in a number of experimental (refs 11−14 and references therein) or theoretical[15−17] works. In the laboratory, crystals of NAM, NAD, and NAT have been prepared in a variety of conditions,[11−14,17−32] and the individual molecules have also been studied in molecular jets or matrixes.[33,34] A fully comprehensive understanding of the spectroscopic characteristics of these species, however, is not yet achieved, partly because most of the theoretical studies deal with the individual molecules and their water aggregates, and not on the crystals or solids that the hydrates form. As far as we know, the only theoretical works that specifically deal with the solids are by Poshusta et al.[35] and Toth[15] on the monohydrate, and by Sullivan et al.[16] on the trihydrate, to which can be added a very recent research by Mantz el al[10] on the interaction of HCl with crystalline NAT. All these papers perform ab initio molecular dynamics calculations based on the Car-Parrinello method (CPMD). Toth[15] and Sullivan et al.[16] predict the power spectra at the optimized geometry of the crystals.

The recently developed program SIESTA[36,37] (Spanish Initiative for Electronic Simulation of Thousands of Atoms) allows the ab initio study of periodic systems of large size, by a method that scales linearly in time and computer memory requirements with the number of atoms in a simulation cell. After optimization of the geometry of the periodic structure, atomic forces are calculated, and ancillary programs can calculate the vibrational frequencies of the molecules within the cell, and provide a description of the Cartesian displacements of the atoms in every vibrational mode, which allows in most cases the assignment of the vibrations. This program is therefore appropriate for the simulation of the crystals of nitric acid hydrates.

We present in this article the calculated theoretical structure of NAM, NAD, and NAT crystals, obtained by application of this numerical method. The interest in this optimized geometrical structure lies both in its comparison to the experimental geometry, when it is available, and also in that it provides the basis for further calculations on these systems, like eventual studies on the reactivity of their surfaces, of key importance in atmospheric chemistry, or like the prediction of their infrared spectra, which again can be compared to experimental measurements. In the first section we present a brief discussion of the numerical method. In the following sections, the results on the structure of NAM, NAD, and NAT are described. Then we propose the assignment of the observed spectra, based on the predicted vibrations of the optimized crystal structures, and discuss the assignment with those previously available in the literature.

Numerical Method and Results

A detailed description of the SIESTA program and some of its applications can be found elsewhere.[36,38] We just outline here some of the more important characteristics of the method, and the specific options used in this work. Among other features, the program performs ab initio calculations to optimize the geometry of a number of molecular species contained within a simulation cell, whose dimensions can also be varied in the refinement process. The electronic state is described using density-functional theory (DFT), with either local density (LDA) or generalized gradient (GGA) approximation. Instead of using plane waves as in other methods of application to solids (such as CASTEP [see http://www.tcm.phy.cam.ac.uk/castep/], for example), this program works with wave functions described as linear combinations of numerical atomic orbitals (LCAO). The orbitals are strictly localized, so that the basis functions become zero after a cutoff radius. The cutoff value is expressed in energy units, and corresponds to the excitation energy arising

* Corresponding author. Phone: (34) 91901609. Fax: (34) 915855184. E-mail: rescribano@iem.cfmac.csic.es.

† In memoriam.

10.1021/jp034230m CCC: $25.00
Published on Web 08/23/2003

TABLE 1: Relevant Parameters of the Nitric Acid Hydrates Crystals[a,b]

		NAM	NAD I (Mol. A)	NAD I (Mol. B)	NAD II (Mol. A)	NAD II (Mol. B)	NAT
NO_3^-							
N−O1, N−O2, N−O3	exp.	1.252,1.251,1.249	1.286,1.222,1.235	1.279,1.223,1.253	1.263,1.265,1.214	1.278,1.247,1.226	1.244,1.252,1.251
	calc.	1.283,1.272,1.271	1.314,1.250,1.273	1.308,1.248,1.283	1.288,1.297,1.251	1.306,1.283,1.252	1.271,1.291,1.272
O1NO2, O2NO3, O3NO1	exp.	120.0,120.0,119.9	119.2,123.5,117.4	119.7,122.3,118.0	117.8,121.2,121.0	117.8,122.1,120.2	120.7,118.5,120.7
	calc.	120.8,119.8,119.4	119.7,122.8,117.6	119.2,122.6,118.2	116.9,121.4,121.7	116.6,122.7,120.7	119.8,118.6,121.6
H_3O^+							
O−H1, O−H2, O−H3	exp.	0.93, 0.87, 0.97	0.99, 0.93, 0.81	0.92, 0.91, 0.85	1.00, 0.88, 0.74	0.89, 0.85, 0.82	0.82, 0.86, 0.88
	calc.	1.05, 1.03, 1.04	1.04, 1.04, 1.03	1.02, 1.14, 1.02	1.05, 1.05, 1.03	1.02, 1.11, 1.03	1.12, 1.02, 1.03
H1OH2, H2OH3, H3OH1	exp.	103, 115, 107	111, 108, 117	111, 110, 114	114, 117, 110	111, 111, 109	105, 103, 115
	calc.	108, 110,107	110,113,109	108, 114, 106	114,113,111	109, 111, 106	111, 110, 109
H-bond							
O···H, O···O (NO_3^-, H_3O^+)	exp.	1.71, 2.590	1.55, 2.550	1.69, 2.606	1.53, 2.521	1.76, 2.640	1.78, 2.626
	calc.	1.57, 2.607	1.53, 2.567	1.59, 2.614	1.50, 2.541	1.62,2.640	1.62, 2.639
O···H, O···O (H_2O,H_3O^+)	exp.		1.64, 2.559	1.55, 2.460	1.68, 2.553	1.60, 2.458	1.71, 2.576
	calc.		1.53, 2.568	1.31, 2.448	1.51, 2.559	1.35, 2.462	1.55, 2.579
O···H, O···O (H_2O,H_3O^+)	exp.						1.59, 2.482
	calc.						1.32, 2.439
O···HO (NO_{3-}, $H3O^+$)	exp.	168	172	174	171	177	177
	calc.	179	175	177	172	176	175
O···HO (H_3O^+,H_2O)	exp.		174	176	175	178	171
	calc.		178	176	174	179	174
O···HO (H_3O^+,H_2O)	exp.						177
	calc.						175
Interlayer							
O- - -O (H_3O^+)	exp.	3.122	3.189		3.581		
	calc.	3.126	3.188		3.603		
O- - -O (NO_{3-})	exp.	3.148	3.764		3.435		
	calc.	3.131	3.760		3.406		
H...O (H-bond)	exp.		2.14		2.09		
	calc.		1.98		1.89		
O- - - -O (H-bond)	exp.		2.940		2.884		
	calc.		2.931		2.890		

[a] References for experimental data: NAM: 41,42; NAD I: 42; NAD II: 43; NAT: 42,44. [b] Calculated results: this work. Interatomic distances in Å, angles in degrees.

from the confinement of the basis orbitals. These features allow the number of computations to scale linearly with the number of atoms.[39] Norm-conserving pseudo-potentials are used for core electrons, and valence wave functions are replaced by pseudo-wave functions that do not oscillate strongly in the core region. In the present investigation, we chose the conjugated gradient method in the optimization process, with double-ζ polarized (DZP) basis functions, and a value of 100 meV for the cutoff radius of the confined orbitals. The Hartree and exchange correlation potentials were calculated at the grid points of a mesh, with mesh cutoff values of 150, 200, or 300 Ry. The higher cutoff values were used in test runs, but it was found that the results did not differ from those achieved with a value of 150 Ry, which was then adopted for all the calculations presented here. The correspondence between the mesh cutoff values of the SIESTA program and the values used in plane waves programs is of a factor of 4, i.e., a cutoff of 50 Ry in a plane waves program gives a precision comparable to 200 Ry with SIESTA. We restricted the calculations of the equilibrium geometry and force constants to the Γ point of the Brillouin zone.[40] The phonon distribution can be extended to other points of the wave-vector space (see below).

We performed several tests in which the unit cell parameters, along with the molecular geometry, were allowed to be refined. In most cases, the refined cell dimensions retained values close to the experimental ones.

After finding the equilibrium configuration, the predicted vibrational frequencies are evaluated. Although the present method does not provide an estimation of the dipole intensity of each normal mode, it is possible to propose the corresponding assignment with the aid of the atomic Cartesian displacements, which can be visualized with some accessible software (like Molden [http://www.cmbi.kun.nl/~schaft/molden/molden.html] of Hyperchem [http://www.hyper.com/]). We summarize in Tables 1 and 2 the more relevant optimized geometrical parameters of the nitric acid hydrate crystals and the assignment of the calculated normal modes, respectively. Details of the calculations and assignments are given in the following sections.

The calculations have been carried out on a two-processor SunBlade 1000 workstation and a SGI Origin 3800 computer. A typical running time for an optimization process took between 12 and 48 h, depending on the structure under study.

NAM

The structure of the crystal of nitric acid monohydrate was first determined by Delaplane et al.[41] and has been recently remeasured by Lebrun et al.[42] It belongs to the orthorhombic system, containing four nitric acid and four water units within the unit cell, of dimensions $a = 6.317$ Å, $b = 8.723$ Å, and $c = 5.477$ Å. All molecular species are ionic (NO_3^-, H_3O^+), with a pseudo-3-fold local symmetry. Thus, there are no water molecules present in this crystal, and the infrared spectrum shows a striking lack of bands in the 3500 cm^{-1} region. Each oxonium ion is linked by hydrogen-bonding to three NO_3^- units, forming quasi-planar layers, with layer separation of the order of 3 Å.

The X-ray geometry was taken as input value for the ab initio calculation. We kept the cell dimensions fixed to the observed values and allowed the refinement of the positions of the atoms within. The converged configuration is depicted in the top panel of Figure 1 (right), where a comparison is presented with the experimental X-ray structure (left). Some of the most relevant interatomic distances and angles are presented in Table 1,

TABLE 2: Calculated Wavenumbers for the Normal Modes of Crystalline NAM, NAD(I), and NAT, and Proposed Assignment to the Predominant Molecular Vibrations

NAM		NAD		NAT	
wavenumber range[a]	predominant vibrations[b]	wavenumber range	predominant vibrations	wavenumber range	predominant vibrations
		3489−3470 (4)	ν_3 (H_2O) a−s	3407−3357 (4)	ν_3 (H_2O) a−s
		3333−3297 (4)	ν_3 (H_2O) a−s + ν_3(H_3O^+) a−s	3307−3201 (8)	ν_1(H_2O) s−s + ν_3(H_2O) a−s
		3179−3136 (8)	ν_3 (H_2O) a−s + ν_3(H_3O^+) + ν_1(H_3O^+)	3154−3105 (4)	ν_3(H_2O) a−s + ν_3(H_3O^+) a−s
		3017−2982 (4)	ν_1(H_3O^+) s−s + ν_3(H_3O^+) a−s	3024−2775 (8)	ν_3(H_3O^+) a−s
		2946−2907 (4)	ν_3 (H_3O^+) a−s		
2864−2829 (4)	ν_1 (H_3O^+) s−s	2801−2763 (4)	ν_1(H_3O^+) s−s		
2547−2282 (8)	ν_3 (H_3O^+) a−s	2610−2454 (8)	ν_3(H_3O^+) a−s		
				1897−1800 (4)	ν($H_5O_2^+$) s
1740−1659 (8)	ν_4 (H_3O^+) a−b	1793−1642 (20)	ν_4(H_3O^+) a−b	1707−1651 (8)	ν_2(H_2O) b + ν_4(H_3O^+) a−b
1496−1383 (8)	ν_3 (NO_3^-) a−s	1574−1435 (16)	ν_3(NO_3^-) a−s + ν_2(H_2O) b + ν($H_5O_2^+$) s	1610−1593 (4)	ν_2(H_2O) b
		1339−1303 (8)	ν_3(NO_3^-) a−s + ν_2(H_3O^+) s−b	1576−1560 (4)	ν_2(H_2O) b + ν_3(H_3O^+) a−s
				1476−1369 (8)	ν_3(NO_3^-) a−s
1326−1177 (4)	ν_2 (H_3O^+) s−b	1295−1263 (4)	ν_2(H_3O^+) s−b + ν_3(NO_3^-) a−s	1319−1306 (4)	ν_2(H_3O^+) s−b
		1213−1181 (4)	ν_2(H_3O^+) s−b		
				1081−1071 (4)	ν_1(NO_3^-)
1135−1130 (4)	ν_1 (NO_3^-) s−s	1054−1043 (8)	ν_1(NO_3^-) s−s	1057−1017 (4)	ν_2(H_3O^+) s−b + ν_2(H_2O) b + ν_1(NO_3^-) s−s

[a] Number in parentheses indicates number of fundamental modes grouped in this range. [b] s-, a-: symmetric or asymmetric; s: stretching, b: bending.

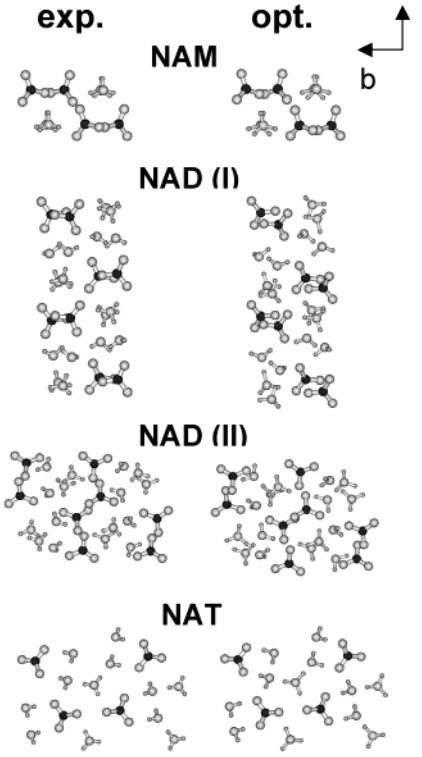

Figure 1. View of the atomic arrangement in a unit cell. Dark circles represent N atoms. Left: experimental X-ray structures from refs 41, 42, 43, and 44, respectively; right: optimized structures, with mesh cutoff value of 150 Ry. Fixed-cell refinements for NAM and NAD, and free-cell optimization for NAT.

compared with the experimental observations of refs 41 and 42. The N−O atomic distances are quite well reproduced, as are the near-C_3-symmetry angles, with a maximum deviation of only 0.03 Å (0.05 Å for an intermolecular pair of atoms). The agreement on the H_3O^+ parameters is less satisfactory, with a maximum deviation of 0.2 Å, which is of the order of three times the accuracy with which the position of the H atoms is estimated from the X-ray measurements. The hydrogen-bond and interlayer parameters are again remarkably well reproduced. The values calculated by Tóth[15] for the bulk NAM crystal are in the same range, although his N−O distances seem slightly overestimated.

NAD

Two different crystal structures of the dihydrate have been found in the last two years.[42,43] The lower temperature phase, NAD(I), is monoclinic, with cell parameters $a = 17.51$ Å, $b = 7.62$ Å, $c = 6.25$ Å, and $\alpha = \gamma = 90°$, $\beta = 107.5°$.[42] It has a layer structure as in NAM, the layers being bound by weak van der Waals forces and weak hydrogen bonds, with interatomic distances of the order of 3−3.5 Å for the former and ∼2 Å for the latter.[42] There are 8 nitric acid units and 8 water pairs in each unit cell. All nitric structures are ionic, but the water units appear as either $H_5O_2^+$, or H_3O^+ and H_2O, linked by a hydrogen bond. Two independent dihydrate molecular structures can be identified in each cell, denoted A and B. The local symmetry of the NO_3^- units, which are planar, is no longer 3-fold, which has given rise to discussions concerning the splitting of otherwise degenerate vibrational bands (see below).

The molecular composition and distribution of the higher temperature phase, NAD(II), is similar, but the cell parameters are quite different: $a = 9.67$ Å, $b = 12.92$ Å, $c = 6.48$ Å, and $\alpha = \gamma = 90°$, $\beta = 97.7°$.[43] We have simulated both phases, with the results shown in the middle panels of Figure 1 and in Table 1. As far as we know, this is the first calculation to be published on the structure of the nitric acid dihydrate crystal. The structural variations from the X-ray geometry after refinement followed the same trend as for the monohydrate, with maximum O−H deviations of ∼0.25 Å, and notable agreement on bending angles and interlayer separation distances.

NAT

The trihydrate crystal has orthorhombic symmetry, with $a = 9.48$ Å, $b = 14.68$ Å, and $c = 3.43$ Å.[44] Unlike the other hydrates, there is no clear layer structure, and all units are linked by three-dimensional hydrogen bonds. In the experimentally determined structure, the completely ionized NO_3^- units have 3-fold local symmetry, and the water units appear as an H_3O^+

ion with one H_2O molecule at either side, linked by weak hydrogen bonds. There are 4 nitrate and 4 $H_3O^+(H_2O)_2$ units in each unit cell. The bottom panel of Figure 1 presents a view of this crystal. As before, the left graph corresponds to the experimental X-ray structure, taken as input for the geometrical optimization. The standard calculations with the SIESTA program yielded in this case two structures which were not quite satisfactory. When the unit cell dimensions were fixed, the variations in the atomic positions after the refinement were larger than for the previous hydrates, with one N−O bond substantially longer than the other two (1.34 Å to be compared to 1.24 and 1.26 Å). This broke the C_3 local symmetry of NO_3^- and induced a rotation of the associated water molecule, which made the structure appear quite different from the observed one. On the other hand, when the cell dimensions were released, the local symmetry of the NO_3^- was maintained, but the size of the unit cell was substantially increased, with a large increment in the *b* and *c* axes, yielding a volume enhancement of more than 30%. We therefore decided to choose a $1 \times 1 \times 3$ supercell as the simulation cell. This calculation helped to stabilize the structure, yielding a volume variation of only 3%, and a refined molecular geometry of comparable quality to that obtained for the other hydrates. The central cell of the 3-cell structure is depicted in Figure 1. The most relevant parameters are shown in Table 1, where it can be seen that all bond lengths and angles agree well with the experimental measurements, with the exception of interatomic distances where the H atom is involved which are reproduced within three times the experimental uncertainty, as for NAM and NAD. Our results coincide also within the estimated uncertainty with those obtained by Sullivan et al.,[16] who performed a CPMD calculation with 3 unit cells as simulation cell as well. To test the convergence of our refinements, we extended the calculations to four *k*-points along the first Brillouin zone, but the results on atomic distances and angles were practically identical to those of the $k = 0$ point. Since the convergence is therefore achieved, we attribute the remaining differences between observed and calculated geometries either to limitations in the basis set used, which is the largest that the method allows, or to possible inadequacies in the theoretical treatment of van der Waals interatomic forces, which may exist in these systems.

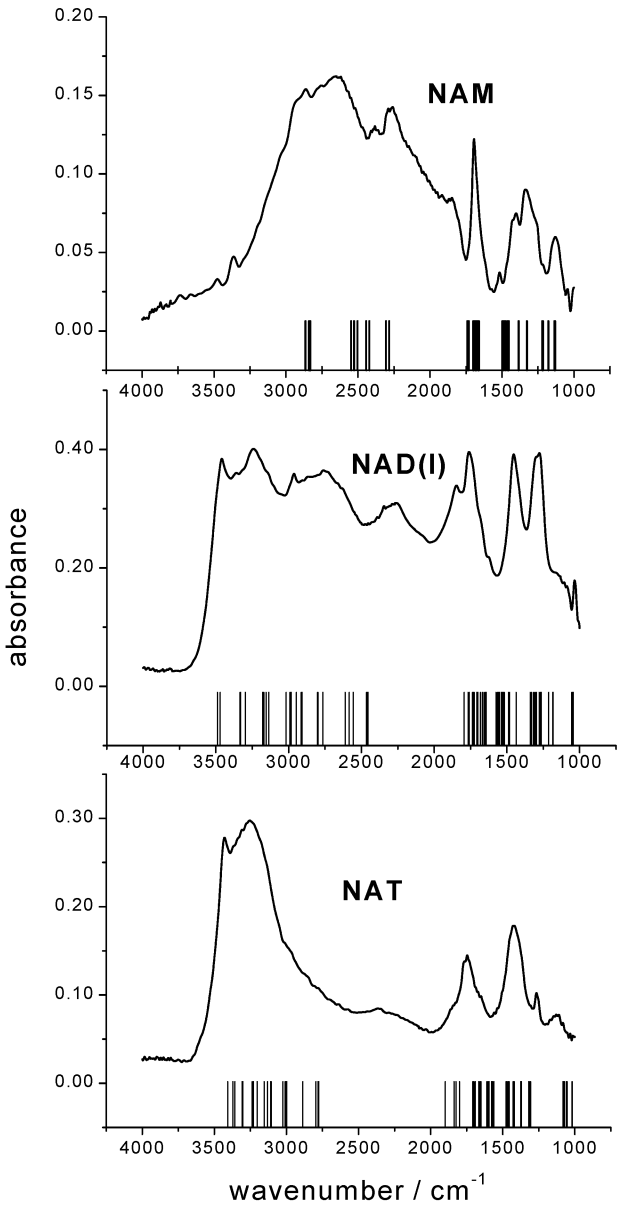

Figure 2. Observed spectra (from ref 14) and predicted normal mode wavenumbers for the nitric acid hydrates. All predicted vibrations are represented as thin lines of unitary height.

Vibrational Spectra

Many experimental groups have reported vibrational spectra of the crystalline nitric acid hydrates generated and measured under different conditions. As discussed in ref 14, despite the large differences found in the relative intensity of the various absorption bands, there is a reasonable agreement between the location of the main absorption maxima, which are the relevant data for comparison with the present calculations. We display in three panels of Figure 2 the spectra of the hydrate crystals measured in our laboratory with our reflection−absorption FTIR setup.[14] At the bottom of each spectrum, we have represented the corresponding calculated normal mode wavenumbers in the 1000−4000 cm^{-1} range. Each predicted wavenumber is represented by a single narrow column of unitary height; therefore, thicker lines indicate groups of vibrations of very close frequency. For illustration, we have also plotted in Figure 3 the dispersion curves for the trihydrate crystal, which afford some information on the grouping of the corresponding normal modes. With the help of these graphs, we have been able to propose an assignment of the observed spectra on the basis of theoretical calculations only. We discuss this assignment in the following paragraphs, and compare it with the measurements and experimental assignments available in the literature (see refs 11, 18, 26, 27, and references therein), which are based on the spectra of other compounds containing oxonium and nitrate ions. A summary of the assignments is presented in Table 2, with an indication of the number of normal modes that take part in each group of calculated vibrations. As indicated above, theoretical predictions of the vibrational frequencies of NAM and NAT based on the CPMD formalism have also been reported by Toth[15] and by Sullivan et al.,[16] respectively. These two calculations propose an approximate assignment of the absorption frequencies corresponding to various molecular modes within the crystal. In general, the present results provide a somewhat better description of the observed spectra, especially in the region of the O−H stretching vibrations. The calculations for NAD presented in this paper provide the first theoretical results to be published on this species.

The atomic Cartesian displacements associated with each calculated frequency show that, in many cases, the corresponding vibrations are in- and out-of-phase combinations of the

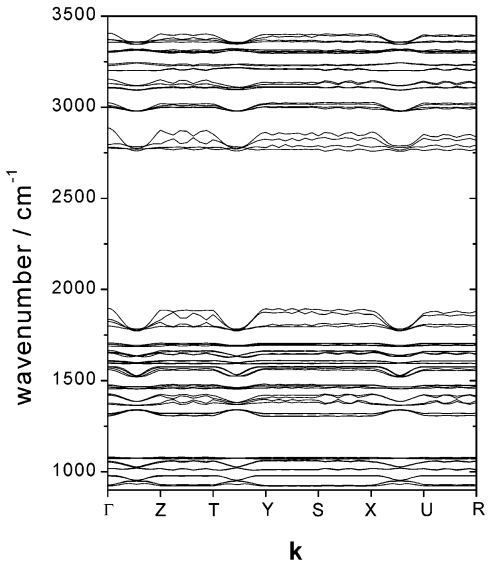

Figure 3. Dispersion curves for the trihydrate.

normal modes of individual molecules of the same type within the unit cell, but there is often a clear contribution from more than one type of molecules. As a general rule, this mixing of vibrations of nonequivalent units grows with the number of water molecules in the hydrates (NAM to NAT). Most vibrations are spread over a wavenumber range of variable span. Thus, the symmetric and antisymmetric stretchings of the water and H_3O^+ units always span more than 500 cm^{-1} and appear at frequencies higher than 2000 cm^{-1}, whereas the bending modes of these molecules, or the stretchings of the NO_3^- units, are much more compressed. For the dihydrate, which has 16 water molecules in the unit cell, the O−H stretchings extend over the largest range, of more than 1000 cm^{-1}. For the three hydrates there is a gap of several hundreds of cm^{-1} between the region of the O−H stretchings and that of the rest of vibrations.

As mentioned above, the observed spectrum of NAM (upper panel of Figure 2) does not show significant absorptions beyond 3000 cm^{-1}, due to the lack of water molecules in its crystal structure.[41,42] The two small peaks appearing between 3200 and 3500 cm^{-1} are most surely due to contamination. Four groups of normal modes are calculated in the region between 2900 and 2300 cm^{-1}. The location of these modes corresponds roughly to that of the peaks appreciable in the broad absorption region above 2000 cm^{-1}. According to the present calculations, the highest frequency peak at about 2850 cm^{-1} corresponds to the O−H symmetric stretching of the H_3O^+ ions. The rest of the absorption peaks are due essentially to O−H asymmetric stretching motions of the hydronium ions. This result is in contrast with some of the experimental assignments,[18,27] which assume that ν_3 (H_3O^+) (asymmetric) > ν_1 (H_3O^+) (symmetric). An inversion in the relative wavenumber values, like the one found here, is also obtained in the CPMD calculations of Sullivan et al.[16] for the NAT crystal. Other assignments or calculations[11,15] do not identify either of the two stretching modes of H_3O^+.

The O−H stretching vibrations of water are present as expected in the normal-mode analysis of the NAD and NAT spectra. In both cases, the calculated highest vibrational frequencies correspond to antisymmetric stretchings of water molecules, ν_3 (H_2O), in a group of four fairly close modes in good coincidence with the highest frequency peaks in the observed spectra. At lower frequencies, down to 2400 cm^{-1}, a combination of water and H_3O^+ symmetric and asymmetric stretchings gives rise to broader absorption features. The corresponding normal modes span a wider frequency range in NAD in accordance with the experimental observations.

For the three hydrates, a series of normal modes associated with the asymmetric bending ("scissors mode") ν_4 of H_3O^+ appear in the 1800−1600 cm^{-1} region in good correspondence with observed absorptions and literature assignments.[11,27] In the case of NAM, the calculated normal modes are concentrated in a frequency interval of less than 100 cm^{-1} corresponding to a comparatively narrow experimental peak. For the dihydrate, the large number of normal modes associated with this bending vibration is spread over a wider frequency range, between 1793 and 1642 cm^{-1}, with a higher density of normal modes toward the low-frequency end of this interval. Experimentally, a broad absorption band is observed between ≈1900 and 1600 cm^{-1}, with a maximum in the lower frequency half of this range. In the trihydrate, these normal modes appear often mixed with bending vibrations of H_2O. These vibrations should account for most of the broad experimental absorption centered at ≈1700 cm^{-1}. In the crystal lattice of NAT, $H_5O_2^+$ units, formed by hydrogen bonding between H_3O^+ and a neighboring water molecule, can be identified. The shared hydrogen atom can oscillate between the two oxygen atoms giving rise to a characteristic vibration denoted $\nu(H_5O_2^+)$ in Table 2, which could also be described as a mixture of $\nu_1(H_2O)$ and $\nu_3(H_3O^+)$. This vibration, predicted in the 1800−1900 cm^{-1} range, can also contribute to the higher frequency part of the experimental band observed at ≈1700 cm^{-1}.

The asymmetric stretching vibrations of the nitrate ion, $\nu_3(NO_3^-)$, appear always below 1550 cm^{-1}. In the monohydrate the calculations yield eight normal modes with predominance of this vibration that can contribute to the observed absorption band between 1500 and 1200 cm^{-1}, although the calculated frequencies are higher than those of the observed maximum (≈1300 cm^{-1}). One of the most characteristic features of the NAD spectra is the splitting of this otherwise degenerate vibration, commonly attributed to the asymmetric surrounding of the NO_3^- ion in the dihydrate crystal.[11,26] This splitting is corroborated in the present theoretical prediction, where the modes in which $\nu_3(NO_3^-)$ is predominant appear in two groups separated by a gap. These two groups of frequencies are somewhat blue shifted with respect to the experimental absorption maxima. The analysis of the molecular motions in the unit cell shows that this vibration is always mixed to a greater or lesser extent with $\nu(H_5O_2^+)$ and with the symmetric bending of hydronium, $\nu_2(H_3O^+)$. The experimental NAT spectrum shows a clear gap at about 1600 cm^{-1}. The theoretical predictions present also a frequency gap, with H_2O bendings predominant in the upper zone (1560−1576 cm^{-1}), and $\nu_3(NO_3^-)$ preponderant between 1369 and 1476 cm^{-1}, this last zone being in very good agreement with the position of the observed experimental peak (around ≈1400 cm^{-1}).

Symmetric bending vibrations ("umbrella mode") of hydronium, $\nu_2(H_3O^+)$ are predicted at frequencies below 1350 cm^{-1}. In NAM, part of these modes might contribute to the absorption band between 1200 and 1500 cm^{-1}, and another part could explain the observed peak at ≈1130 cm^{-1}. In NAD the modes predominantly due to $\nu_2(H_3O^+)$ are located between 1295 and 1181 cm^{-1}, with mixing with $\nu_3(NO_3^-)$ in the higher part of this range, and approximate agreement of the lower part of the interval with the experimental shoulder at ≈1200−1100 cm^{-1}. In the trihydrate, the $\nu_2(H_3O^+)$ vibrations appear around 1300 cm^{-1} and should contribute to the large experimental absorption centered at ≈1400 cm^{-1}, mentioned in the previous paragraph,

in contrast with current literature assignments,[11,27] which attribute this band exclusively to $\nu_3(NO_3^-)$.

Normal modes containing symmetric stretching vibrations of the nitrate ion, $\nu_1(NO_3^-)$, are only found for frequencies lower than 1140 cm^{-1}. Due to the D_{3h} symmetry of the isolated ion, the N−O symmetric stretch would be infrared inactive in the gas phase. In a crystal, this vibration will become active in a local environment without 3-fold symmetry, through interactions with the other molecular units of the unit cell. In the NAD crystal,[42,43] the NO_3^- ion is not symmetric and this vibration is expected to be active. The present calculations yield, for this crystal, a set of eight $\nu_1(NO_3^-)$ normal modes closely packed between 1054 and 1043 cm^{-1}, in very good agreement with the experimental narrow peak currently assigned to this vibration.[11,18,26,27] Although NO_3^- is quasi-symmetric in NAM and NAT, the consideration of vibrations for the whole unit cell suggests that some of these stretching modes should become active. In NAM, the predicted frequencies are however close to those of $\nu_2(H_3O^+)$ and it is not possible to determine whether they contribute to the observed absorptions, as suggested by Tso and Leu.[27] In NAT the modes in which $\nu_1(NO_3^-)$ is predominant appear at 1081−1071 cm^{-1}; between 1057 and 1017 cm^{-1} the nitrate vibrations are mixed with more complicated bending motions involving simultaneously water and H_3O^+ units. At a somewhat larger frequency ($\approx$1120 cm^{-1}) there is an experimental absorption feature attributed in the bibliography either to $\nu_2(H_3O^+)$[11] or to $\nu_1(NO_3^-)$.[27] This feature, however, is not present in all the published spectra and seems to be strongly dependent on the conditions of formation of the hydrate.[12]

The appearance of experimental absorptions, namely a shoulder at 1850 cm^{-1} for NAM, a band at $\approx$ 2260 cm^{-1} for NAD, and a broad weak band at $\approx$2350 cm^{-1} for NAT, in the gap between the O−H stretchings and the rest of the modes, is worth noting. These features are present with more or less intensity in most of the literature spectra, but they are usually not assigned, with the exception of the NAD peak which has been attributed to a stretching vibration of H_3O^+.[11,26,27] The absence of predictions for these bands, and the existence of similar gaps in the CPMD calculations of Toth[15] and of Sullivan et al.[16] for NAM and NAT, respectively, suggest that the observed absorptions (or some of them) may be due to second-order modes.

Conclusions

The crystalline structure of the nitric acid hydrates, species of key relevance in atmospheric processes, has been determined by application of the ab initio program SIESTA. From the refined geometry and force constants of these crystals, we have calculated their vibrational normal modes. The analysis of these normal modes provides an adequate tool to discuss the assignment of the spectra. We have found in general a good agreement with the observed spectra, being particularly successful the assignment of the asymmetric stretching modes of H_2O in NAD and NAT, the splitting of the asymmetric stretching of NO_3^- in NAD, and the symmetric stretching vibration of NO_3^- in this same crystal, characterized by a narrow peak, whose location is precisely matched. It may be emphasized that the optimized crystal structure and vibrational assignment of both phases of NAD are presented here for the first time.

Acknowledgment. This investigation has been funded by the Spanish Ministry of Science and Technology, Project REN2000-1557. We acknowledge CIEMAT for use of their computing facilities.

References and Notes

(1) Rowland, F. S. *Annu. Rev. Phys. Chem.* **1991**, *42*, 731.
(2) Solomon, S. *Nature* **1990**, *347*, 347.
(3) Molina, M. J.; Tso, T.-L.; Molina, L. T.; Wang, F. C.-Y. *Science* **1987**, 1253.
(4) Salcedo, D.; Molina, L. T.; Molina, M. J. J. *J. Geophys. Res. Lett.* **2000**, *27*, 193.
(5) Voigt, C.; Schreiner, J.; Kohlmann, A.; Zink, P.; Mauersberger, K.; Larsen, N.; Deshler, T.; Kröger, C.; Rosen, J.; Adriani, A.; Cairo, F.; Di Donfrancesco, G.; Viterbini, M.; Ovarlez, J.; Ovarlez, H.; David, C.; Dörnbrack, A. *Science* **2000**, 1756.
(6) Larsen, N.; Mikkelsen, I. S.; Knudsen, B. M.; Screiner, J.; Voigt, C.; Mauersberger, K.; Rosen, J. M.; Kjome, N. T. *J. Geophys. Res.* **2000**, *105*, 1491.
(7) Zondlo, M. A.; Hudson, P. K.; Prenni, A. J.; Tolbert, M. A. *Annu. Rev. Phys. Chem.* **2000**, *51*, 473.
(8) Bertram, A. K.; Dickens, D. B.; Sloan, J. J. *J. Geophys. Res.* **2000**, *105*, 9283.
(9) Salcedo, D.; Molina, L. T.; Molina, M. J. *J. Phys. Chem. A* **2001**, *105*, 1433.
(10) Mantz, Y. A.; Geiger, F. M.; Molina, L. T.; Molina, M. J.; Trout, B. L. *J. Phys. Chem. A* **2002**, *106*, 6972.
(11) Ritzhaupt, G.; Devlin, J. P. *J. Phys. Chem.* **1991**, *95*, 90.
(12) Tisdale, R. T.; Prenni, A. J.; Iraci, L. T.; Tolbert, M. A.; Toon, O. B. *Geophys. Res. Lett.* **1999**, *26*, 707.
(13) Sato, M.; Setokuchi, O.; Yamada, K. M. T.; Ibusuki, T. *Vib. Spectrosc.* **2002**, *956*, 1.
(14) Escribano, R.; Couceiro, M.; Gómez, P. C.; Carrasco, E.; Moreno, M. A.; Herrero, V. J. *J. Phys. Chem. A* **2003**, *107*, 651.
(15) Tóth, G. *J. Phys. Chem. A* **1997**, *101*, 8871.
(16) Sullivan, D. M.; Bagchi, K.; Tuckerman, M. E.; Klein, M. I. *J. Phys. Chem. A* **1999**, *103*, 8678.
(17) Staikova, M.; Donaldson, D. J. *Phys. Chem. Chem. Phys.* **2001**, *3*, 1999.
(18) Smith, R. H.; Leu, M.-T.; Keyser, L. F. *J. Chem. Phys.* **1991**, *95*, 5924.
(19) Koehler, B. G.; Middlebrook, A. M.; Tolbert, M. A. *J. Geophys. Res.* **1992**, *97*, 8065.
(20) Tolbert, M. A.; Koehler, B. G.; Middlebrook, A. M. *Spectrochim. Acta* **1992**, *48A*, 130.
(21) Barton, N.; Rowland, B.; Devlin, J. P. *J. Phys. Chem.* **1993**, *97*, 5848.
(22) Toon, O. B.; Tolbert, M. A.: Koehler, B. G.; Middlebrook, A. M.; Jordan, J. *J. Geophys. Res.* **1994**, *99*, 25631.
(23) Schrems, O.; Peil, S. *Heterogeneous and Homogeneous Chemistry of ClO_y, BrO_y, and NO_y Compounds on Polar Stratospheric Cloud Mimics. CEC Report for STEP Programme CT-90-0071*; 1993. The RAIR spectra of the nitric acid hydrates are shown in Figure 2 of Sodeau, J. R. Atmospheric Cryochemistry. In *Spectroscopy in Enviromental Science*; Clark, R. H. J.; Lester, R. E., Eds.; John Wiley and Sons: New York, 1995.
(24) Peil, S.; Seisel, S.; Schrems, O. *J. Mol. Struct.* **1995**, *348*, 449.
(25) Richwine, J. L.; Clapp, M. L.; Miller, R. E.; Worsnop, D. R. *Geophys. Res. Lett.* **1995**, *22*, 2625.
(26) Koch, T. G.; Holmes, N. S.; Roddis, T. B.; Sodeau, J. R. *J. Chem. Soc., Faraday Trans.* **1996**, *92*, 4787.
(27) Tso, T.-L.; Leu, M.-T. *Anal. Sci.* **1996**, *12*, 615.
(28) Dieselkamp, R. S.; Anthony, S. E.; Prenni, A. J.; Onasch, T. B.; Tolbert, M. A. *J. Phys. Chem.* **1996**, *100*, 9127.
(29) Tisdale, R. T.; Middlebrook, A. M.; Prenni, A. J.; Tolbert, M. A. *J. Phys. Chem. A* **1997**, *101*, 2112.
(30) Niedziela, R. F.; Miller, R. E.; Worsnop, D. R. *J. Phys. Chem. A* **1998**, *102*, 6477.
(31) Bertram, A. K.; Sloan, J. J. *J. Geophys. Res.* **1998**, *103*, 3553.
(32) Bertram, A. K.; Sloan, J. J. *J. Geophys. Res.* **1998**, *103*, 13265.
(33) Canagaratna, M.; Phillips, J. A.; Ott, M. E.; Leopold, K. R. *J. Phys. Chem. A* **1998**, *102*, 1489.
(34) McCurdy, P. R.; Hess, W. P.; Xantheas, S. *J. Phys. Chem. A* **2002**, *106*, 7628.
(35) Poshusta, R. D.; Tseng, D. C.; Hess, A. C.; McCarthy, M. I. *J. Phys. Chem.* **1993**, *97*, 7295.
(36) Soler, J. M.; Artacho, E.; Gale, J. D.; García, A.; Junqure, J.; Ordejón, P.; Sánchez-Portal, D. *J. Phys.: Condens. Matter* **2002**, *14*, 2745.
(37) Artacho, E.; Sánchez-Portal, D.; Ordejón, P.; García, A.; Soler, J. M. *Phys. Status Solidi* **1999**, *215*, 809.
(38) Sainz-Diaz, C. I.; Timón, V.; Botella, V.; Artacho, E.; Hernández-Laguna, A. *Am. Mineral.* **2002**, *87*, 958.

(39) Sánchez-Portal, D.; Ordejón, P.; Artacho, E.; Soler, J. M. *Int. J. Quantum Chem.* **1997**, *65*, 453.
(40) Stich, I.; Parrinello, M.; Holender, J. M. *Phys. Rev. Lett.* **1996**, *76*, 2077.
(41) Delaplane, R. G.; Taesler, I.; Olovsson, I. *Acta Crystallogr.* **1975**, *B31*, 1486.
(42) Lebrun, N.; Mahe, F.; Lamiot, J.; Foulon, M.; Petit, J.; Prevost, D. *Acta Crystallogr.* **2001**, *B57*, 27.
(43) Lebrun, N.; Mahe, F.; Lamiot, J.; Foulon, M.; Petit, J. *Acta Crystallogr.* **2001**, *C57*, 1129.
(44) Taesler, I.; Delaplane, R. G.; Olovsson, I. *Acta Crystallogr.* **1975**, *B31*, 1489.